


RESEARCH ARTICLE

LCP1 triggers mTORC2/AKT activity and is pharmacologically targeted by enzastaurin in hypereosinophilia

Guangxin Ma^{1,2} | Deniz Gezer¹ | Oliver Herrmann¹ | Kristina Feldberg¹ |
Mirle Schemioneck¹ | Mohamad Jawhar³ | Andreas Reiter³ | Tim H. Brümmendorf¹ |
Steffen Koschmieder¹ | Nicolas Chatain¹ 

¹Department of Hematology, Oncology, Hemostaseology, and Stem Cell Transplantation, Faculty of Medicine, RWTH Aachen University, Aachen, Germany

²Hematology and Oncology Unit, Department of Geriatrics, Qilu Hospital of Shandong University, Jinan, Shandong, China

³Department of Hematology and Oncology, University Medical Centre Mannheim, Heidelberg University, Mannheim, Germany

Correspondence

Nicolas Chatain, Department of Hematology, Oncology, Hemostaseology, and Stem Cell Transplantation, Faculty of Medicine, RWTH Aachen University, Pauwelsstr 30, D-52074 Aachen, Germany.
Email: nchatain@ukaachen.de

Funding information

China Scholarship Council, Grant/Award Number: 201406220165; BILD hilft e.V. "Ein Herz für Kinder", Grant/Award Number: PÄ-13311

Abstract

Hypereosinophilia (HE) is caused by a variety of disorders, ranging from parasite infections to autoimmune diseases and cancer. Only a small proportion of HE cases are clonal malignancies, and one of these, the group of eosinophilia-associated tyrosine kinase fusion-driven neoplasms, is sensitive to tyrosine kinase inhibitors, while most subtypes lack specific treatment. Eosinophil functions are highly dependent on actin polymerization, promoting priming, shape change, and infiltration of inflamed tissues. Therefore, we investigated the role of the actin-binding protein lymphocyte cytosolic protein 1 (LCP1) in malignant and nonmalignant eosinophil differentiation. We use the protein kinase C- β (PKC β) selective inhibitor enzastaurin (Enza) to dephosphorylate and inactivate LCP1 in FIP1L1-platelet-derived growth factor receptor α (PDGFRA)-positive EoL-1 cells, and this was associated with reduced proliferation, metabolic activity, and colony formation as well as enhanced apoptosis and impaired migration. While Enza did not alter FIP1L1-PDGFRA-induced signal transducer and activator of transcription 3 (STAT3), STAT5, and ERK1/2 phosphorylation, it inhibited STAT1^{Tyr701} and AKT^{Ser473} (but not AKT^{Thr308}) phosphorylation, and short hairpin RNA knockdown experiments confirmed that this process was mediated by LCP1 and associated mammalian target of rapamycin complex 2 (mTORC2) activity loss. Homeobox protein HoxB8 immortalized murine bone marrow cells showed impaired eosinophilic differentiation upon Enza treatment or LCP1 knockdown. Furthermore, Enza treatment of primary HE samples reduced eosinophil differentiation and survival. In conclusion, our data show that HE involves active LCP1, which interacts with mTOR and triggers mTORC2 activity, and that

Abbreviations: Enza, enzastaurin; F/P, Fip1L1-PDGFRA; FACS, fluorescence activated cell sorting; FBS, fetal bovine serum; GAPDH, glyceraldehyde 3-phosphate dehydrogenase; GFP, green fluorescent protein; HE, hypereosinophilia; HES, hypereosinophilic syndrome; HoxB8, Homeobox protein Hox-B8; HRP, horseradish peroxidase; IL-3, interleukin-3; IL-5, interleukin-5; kDa, kilodalton; MNC, mononuclear cells; MPN, myeloproliferative neoplasms; MTT, 3-(4,5-dimethylthiazol-2-yl)-2,5-diphenyltetrazolium bromide; mTOR, mammalian target of rapamycin; mTORC2, mTOR complex 2; PDGF, platelet-derived growth factor receptor; PDK1, Pyruvate dehydrogenase lipoamide kinase isozyme 1; PI3K, phosphatidylinositol 3-kinase; PKC, protein kinase C; RFP, red fluorescent protein; SCF, stem cell factor; STAT, signal transducer and activator of transcription; TKI, tyrosine kinase inhibitor.

Steffen Koschmieder and Nicolas Chatain contributed equally to this study.

This is an open access article under the terms of the Creative Commons Attribution License, which permits use, distribution and reproduction in any medium, provided the original work is properly cited.

© 2019 The Authors. *Molecular Carcinogenesis* published by Wiley Periodicals, Inc.

the PKC β inhibitor Enza as well as targeting of LCP1 may provide a novel treatment approach to hypereosinophilic disorders.

KEYWORDS

differentiation block, hypereosinophilia, LCP1, mTORC2, myeloid neoplasms

1 | INTRODUCTION

Hypereosinophilia (HE) is defined by an increase of circulating eosinophils above 1500/ μ L, and can be accompanied by extensive bone marrow and tissue infiltration as well as eosinophil granule protein deposition.¹ The most common underlying conditions of reactive HE include infection, allergy, medication, and autoimmune disorders,² and these are mostly mediated by eosinophilopoietic cytokines (interleukin-3 [IL-3], IL-5, GM-CSF).² Clonal HE can be associated with myeloid neoplasms such as chronic myeloid leukemia (CML), acute myeloid leukemia (AML), chronic eosinophilic leukemia, or systemic mastocytosis, and is genetically classified according to the new revised WHO classification from 2016.³ The latter subgroup includes clonal HE associated with tyrosine kinase fusion proteins involving the platelet-derived growth factor receptor α (PDGFRA) and PDGFRB, which are sensitive to the tyrosine kinase inhibitor (TKI) imatinib and have a favorable prognosis, or the fibroblast growth factor receptor 1 fusion.⁴ However, most HE cases lack such fusion proteins, and, thus, new treatments are needed for these patients, particularly since standard therapy with steroids is associated with significant long-term side effects.

The actin cytoskeleton and associated proteins play important roles in eosinophil signaling, motility, degranulation, phagocytosis, and activation.⁵⁻⁷ Eosinophils harbor high amounts of actin and actin dynamic modulators.⁸ Lymphocyte cytosolic protein 1 (LCP1, L-plastin), an actin-binding protein and downstream target of the serine/threonine kinase protein kinase C (PKC) β II, mediates eosinophil priming.⁹ While LCP1 is ubiquitously expressed in all hematopoietic lineages, it is strongly upregulated in many tumor cells, making LCP1 a potential prognostic factor.¹⁰⁻¹² Its phosphorylation at the regulatory serine 5 (Ser5) residue can be stimulated by several factors, including CXCL12,¹³ GM-CSF,⁹ and fMLP,¹⁴ thereby manipulating F-actin bundling¹⁵ and integrin expression.⁹ In atopic dermatitis, the epithelial cytokine thymic stromal lymphopoietin activates LCP1 and induces eosinophil migration, which is abrogated by PKC β inhibition. PKC β belongs to the classic PKC family of proteins. It consists of two isoforms, PKC β I and PKC β II, generated by alternative splicing.¹⁶ PKC β was shown to be overexpressed in several solid tumors, including colon, breast, and prostate cancer.¹⁷⁻¹⁹ In the hematopoietic system, PKC β has been associated with monocytic chemotaxis and chronic lymphocytic leukemia cell proliferation.^{20,21} In eosinophils, PKC β is involved in priming, adhesion, shape change, chemotaxis, superoxide generation, and mediator release.²²

Here, we describe the actin-binding protein LCP1 to be crucial for activation of the mammalian target of rapamycin complex 2 (mTORC2) complex and phosphorylation of AKT^{Ser473}, thereby regulating malignant and nonmalignant eosinophil differentiation and survival. In addition, we evaluated the efficacy of enzastaurin (Enza), a specific inhibitor of PKC β ,

in promoting apoptosis and reducing differentiation of eosinophilic cells and the role of LCP1 in this process. Our data suggest that inhibition of LCP1 activity may be used therapeutically in HE patients.

2 | MATERIALS AND METHODS

2.1 | Primary patient samples

HE patient samples were collected in the Department of Hematology, Oncology, Hemostaseology, and Stem Cell Transplantation, RWTH Aachen University and in the Department of Hematology and Oncology, University Medical Center Mannheim, Heidelberg University (Table 1). Patients were diagnosed with HE/hypereosinophilic syndrome (HES) according to the WHO criteria 2016.³ The sample collection was approved by the local ethics boards of the Medical Faculty of RWTH Aachen University and of the University Medical Center Mannheim. Informed consent was obtained from all patients.

2.2 | Reagents and antibodies

The PKC β -specific inhibitor Enza (LY317615) and the pan-PKC inhibitor sotrastaurin were purchased from Selleckchem (Munich, Germany). The murine F/P vector was provided by Prof. Jan Cools, University of Leuven, Belgium. Phospho-LCP1 (Ser5) antibody¹⁵ was a kind gift from Dr. Elizabeth Schaffner-Reckinger, University of Luxembourg. Antibodies detecting phospho-STAT5 (Tyr694), phospho-STAT3 (Tyr705), phospho-Sin1 (Thr86), phospho-STAT1 (Tyr701), phospho-ERK1/2 (Thr202/Tyr204), phospho-PDK1 (Ser241), phospho-AKT1/2 at Ser473 or Thr308, Sin1, STAT1, STAT3, PARP-1, ERK1/2, G β L, mTOR, and phospho-AKT substrate were purchased from Cell Signaling Technology (Beverly, MA). Antibodies against STAT5, LCP1, glyceraldehyde 3-phosphate dehydrogenase (GAPDH), β -catenin, c-Jun, and AKT1/2 were obtained from Santa Cruz Biotechnology (Santa Cruz, CA). Polyclonal goat anti-rabbit (P0448), polyclonal rabbit anti-goat (P0160), and polyclonal goat anti-mouse Immunoglobulins/horseradish peroxidase (HRP) (P0447) antibodies were purchased from DAKO (Hamburg, Germany). Siglec-F-APC antibody and the respective immunoglobulin G (IgG) control were obtained from Miltenyi Biotec (Bergisch Gladbach, Germany). CD11b-PB, Siglec-8-APC, CCR3-PE, and IgG controls were purchased from Biolegend (San Diego, CA).

2.3 | DNA constructs and vectors

The cDNA of the Fip1l1-Pdgfra (F/P) fusion gene was cloned into a pMSCV-IRES-GFP vector. The establishment of the pMSCV-LTR-

TABLE 1 Patient baseline data

Patient	Diagnosis	Sex	Age	Current Treatment	Mutation	WBC [10E9/L]	Eosinophil [%]	% positive by FACS on Day 8/9	
								Siglec-8 ⁺ /CCR3 ⁺	Siglec-8 ⁺ /CCR3 ⁺ (enzataurin)
1	Lung cancer	F	57	None	No mutation found	5.9	19.2	90.78	69.30
2 ^a	CEL	M	49	Imatinib	Fip1L1-PDGFRA	6.9	51.4	78.88	45.42
3	HES	M	65	None	No mutation found	8.5	56.0	95.97	48.50
4	HES	M	28	None	No mutation found	8.1	5.5	78.09	68.78
5	HES	M	53	Steroids	No mutation found	5.4	6.5	95.97	69.60
6	HES	F	40	Steroids	No mutation found	19.1	71.2	77.80	48.52
7 ^b	Reactive eosinophilia	M	50	Prednisolone	No mutation found	8.5	6.7	18.03	10.24
8	HES	M	53	Steroids	No mutation found	6.5	4.0	64.96	51.01
9	HES	F	37	Steroids/CSA	No mutation found	8.0	8.7	53.60	45.03
10	ET/Eosinophilia	F	49	None	No mutation found	7.6	5.6	76.67	40.00
11	AML	M	68	Steroids/CSA	ETV6-ABL	16.6	17.3	26.60	39.82
12	CML	F	71	Bosutinib	BCR-ABL	6.6	27.0	86.70	75.12

Abbreviations: CEL, chronic eosinophilic leukemia; DMSO, dimethyl sulfoxide; FACS, fluorescence activated cell sorting; HES, hypereosinophilic syndrome; PDGFRA, platelet-derived growth factor receptor α .
^aStaining was done for Siglec-8.
^bBone marrow.

miR30-SV40 vector was described before.²³ Green fluorescent protein (GFP) was replaced by red fluorescent protein (RFP) in the pMSCV-LTR-miR30-SV40 vector. Three different knockdown sequences of murine LCP1 and scrambled control (Table S1) were designed and cloned into a pMSCV-LTR-miR30-SV40-RFP vector.

2.4 | Cell culture and retroviral transduction

The Fip1l1-Pdgfra fusion gene-positive human cell line Eol-1 and the murine 32Dcl3 (hereafter named as 32D) cells were purchased from DSMZ (Braunschweig, Germany) and cultured in Roswell Park Memorial Institute (RPMI) 1640 medium supplemented with 25 U/mL penicillin/streptomycin and 10% fetal bovine serum (FBS) (all from Thermo Fisher Scientific). The medium for 32D cells was supplemented with 10% WEHI-3B supernatant as IL-3 source. The MSCV-ERHBD-Hoxb8 vector was a gift from Hans Häcker, St. Jude Children's Research Hospital, Memphis, TN. Lineage negative BM cells were isolated from tibia and femur of C57BL/6 J mice (Lineage depletion Kit, Miltenyi Biotech). Cells were immortalized by conditional HOXB8 expression as previously described²⁴ and cultured in Iscove modified Dulbecco medium (Thermo Fisher Scientific) containing 50 ng/mL stem cell factor (SCF) (ImmunoTools, Friesoythe, Germany), 10% FBS, 25 U/mL penicillin/streptomycin, and 1 μ M β -estradiol (Sigma-Aldrich). The retroviral transduction of 32D and Homeobox protein Hox-B8 (HoxB8) immortalized lineage negative murine BM (hereafter named as SCF-ER-HoxB8 BM) cells was described before.²⁵ Cells were fluorescence activated cell sorting (FACS) sorted for GFP or double positivity of GFP and RFP using an Aria cell sorter (BD Bioscience, Heidelberg, Germany).

2.5 | Proliferation assay

Eol-1 cells (2×10^5 /mL) were seeded in the presence of Enza (freshly added every 48 hours). Cell counting was performed at the indicated time points using the CASY Cell Counter (OLS OMNI Life Science, Bremen, Germany) system. Experiments were performed in triplicates.

2.6 | Lentiviral transduction

pMD2.G (Addgene plasmid # 12259), pRSV-Rev (Addgene plasmid # 12253), and pMDLg/pRRE vectors were generated and provided by Didier Trono (Addgene plasmid # 12251). Tet-pLKO-puro was a gift from Dmitri Wiederschain (Addgene plasmid # 21915).²⁶ Tet-pLKO-puro-scrambled was a gift from Charles Rudin (Addgene plasmid # 47541).²⁷ shRNA oligo design and lentiviral transduction protocol was applied as shown before^{28,29} (Table S2). Cells were selected using 500 ng/mL puromycin.

2.7 | Death assay

Eol-1 cells (5×10^5 /mL) were treated with 5 μ M Enza. Apoptotic cells were assessed after 48 or 72 hours incubation by Zombie Aqua staining (Biolegend) according to the manufacturer's protocol, using a

Gallios flow cytometer (Beckman Colter, Krefeld, Germany). Experiments were performed in triplicates.

2.8 | MTT assay

The MTT assay have been described earlier.³⁰ In short, 3×10^4 Eol-1 cells/100 μ L medium were exposed to increasing concentrations of Enza in triplicates. Cell viability was analyzed after 72 hours using 10 μ L MTT (5 mg/mL) solution that was incubated for 4 hours at 37°C followed by isopropanol-HCl cell lysis. Adsorption was measured at 550 nm using a microplate reader (Rayto, RT-2100C). The metabolic process of tetrazolium reduction to formazan reflects the number of viable cells, and this is, therefore, stated accordingly.

2.9 | Migration assay

The migration of Eol-1 cells was analyzed using transwell chambers (5- μ m pore size, Costar). Lower chambers contained RPMI medium supplemented with 20% FCS \pm 50 ng/mL CXCL12a. Eol-1 cells were pretreated with either 5 μ M Enza or dimethyl sulfoxide (DMSO) (0.05%) as a control for 24 hours. Subsequently, 1.5×10^5 Eol-1 cells were loaded into the upper chamber and were allowed to migrate for 4 hours. Experiments were performed in triplicates. Migrated cells were counted using a CASY Cell Counter system. The ratio between migrated cell number and total cell number was calculated as % of input cells.

2.10 | Colony formation assay

Eol-1 cells were pretreated with 5 μ M Enza for 24 hours and seeded at a density of 500 cells/mL into methylcellulose (MethoCult, H4230, STEMCELL Technologies), containing 5 μ M Enza or the same volume of DMSO. Experiments were performed in triplicates. Colony formation was analyzed 4 days after plating using a light microscope.

2.11 | Eosinophil differentiation of SCF-ER-HoxB8 BM cells

Eosinophil differentiation was performed by the withdrawal of β -estradiol from SCF-ER-HoxB8 BM cells. Cells were incubated in the presence of 5 μ M Enza, 10 ng/mL IL-5, and 50 ng/mL SCF. Enza, IL-5, and SCF were freshly added every 48 hours. After 4 days, 5×10^5 cells were analyzed for Siglec-F/CD11b double positivity by flow cytometry (Beckman Colter, Gallios). Parallel experiments without IL-5 supplementation were performed as negative controls and all experiments were performed in triplicates.

2.12 | Human eosinophil isolation and differentiation

Isolation of mature granulocytes or mononuclear cells (MNCs) was performed after Ficoll density gradient centrifugation as previously described.³¹ Eosinophil differentiation was performed in triplicates in Iscove modified Dulbecco medium (Gibco, Paisley, UK) supplemented

with 10% FBS, 50 μ M β -mercaptoethanol, 10 U/mL penicillin, 10 μ g/mL streptomycin, 2 mM glutamine and SCF (50 ng/mL), FLT-3 ligand (50 ng/mL), GM-CSF (10 ng/mL), IL-3 (10 ng/mL), and IL-5 (10 ng/mL) as previously described.³² After 3 days of differentiation, only IL-3 and IL-5 were added. On day 8 or 9, both granulocytic cells and MNCs were stained in the dark at room temperature for 40 minutes with APC-conjugated Siglec-8 and PE-conjugated CCR3 antibody. The cell number of mature granulocytes, isolated from the pellet, was counted by the CASY cell counter.

2.13 | Preparation of cell lysates, sodium dodecyl sulfate-polyacrylamide gel electrophoresis, and immunoblotting

Preparation of cell lysates, sodium dodecyl sulfate-polyacrylamide gel electrophoresis (SDS-PAGE) and immunoblotting was performed as described before.²⁵ In short, cell pellets were lysed in ice-cold radioimmunoprecipitation assay buffer supplemented with protease/phosphatase inhibitors (SIGMAFAST Protease Inhibitor, Sigma-Aldrich), denatured in 1X Laemmli buffer at 65°C for 5 minutes and separated by SDS-PAGE and transferred to polyvinylidene difluoride (PVDF) membrane (GE Healthcare, Frankfurt, Germany). Western blotting was performed overnight in Towbin transfer buffer (3 g Tris, 14.4 g glycine, 5% ethanol per liter ddH₂O) at 100 mA. The PVDF membrane was blocked in 10% BSA in TBST buffer (20 mM Tris-HCl, pH 7.6, 137 mM NaCl, 0.05% Tween). The primary antibody (1:1000) was incubated overnight at 4°C, and the secondary antibody conjugated to HRP (1:2000) for 45 minutes after three times washing. Respective proteins were detected via chemiluminescence (Fusion SL, PeqLab). The ImageJ software was used for protein quantification analysis.

2.14 | Coimmunoprecipitation

Eo1-1 cells were treated with 5 μ M Enza for 16 hours and lysates were prepared using coimmunoprecipitation (CoIP) buffer (10 mM HEPES pH 7.5, 50 mM NaCl, 30 mM Na₄P₂O₇, 50 mM NaF, 5 μ M ZnCl₂, 0.2% vol/vol Triton X-100, 10% glycerol) freshly supplemented with protease/phosphatase inhibitors. mTOR specific antibody (1:50; #2972; Cell Signaling Technology) was added to 1 mg of total protein and rotated at 4°C for 16 hours. Protein A/G PLUS-Agarose (Santa Cruz, sc-2003; 25 μ L) was added to the lysate/antibody suspension and rotated at 4°C for 4 hours. The agarose was washed three times with CoIP buffer and resuspended in 25 μ L of 2X Laemmli buffer. The suspension was denatured at 95°C for 5 minutes and used for SDS-PAGE and Western blotting.

2.15 | Real-time quantitative reverse transcriptase-polymerase chain reaction

RNA isolation was performed by phenol/chloroform (TRIzol, Thermo Fisher Scientific) extraction according to the manufacturer's instruction. One microgram RNA was applied for cDNA synthesis using MMLV reverse transcriptase (Thermo Fisher Scientific). The

quantitative reverse transcriptase-polymerase chain reaction was performed using the 7500 Fast Real-time PCR System (Applied Biosystems, Paisley, UK). SYBR Select Master Mix (Applied Biosystems) was used to evaluate gene expression with the indicated primer pairs (Table S3). Experiments were performed in triplicates. GAPDH was used as a housekeeping gene.

2.16 | Software and statistical analysis

All FACS data were evaluated using FlowJo data analysis software (Treestar). Statistical analysis was performed using GraphPad Prism software. Mann-Whitney *U* test was applied for cell line experiments, and in vitro data from patients were analyzed with Wilcoxon matched-pairs test. Statistical differences were determined by ns—not significant, **P* < .05, ***P* < .01, ****P* < .001. Data are shown as mean and standard deviation. The results are representative for at least three independent experiments.

3 | RESULTS

3.1 | LCP1 regulates AKT and STAT1 phosphorylation downstream of F/P

The PKC β II-activated actin-bundling protein LCP1 was described to be required for eosinophil migration and activation.⁹ Therefore, we explored the involvement of LCP1 in the pathogenesis of HE.

The IL-3-dependent murine cell line 32D is easy to manipulate and a good tool to analyze signaling pathways and scaffolds. Therefore, 32D cells were transduced with either an empty vector (EV) or F/P fusion gene, known to be a driver of HE dependent on IL-5 cytokine expression.^{4,33,34} 32D-F/P cells led to cytokine-independent growth and upregulation of LCP1^{Ser5} phosphorylation and total protein expression (Figure 1A). Phosphorylation of LCP1^{Ser5} was inhibited by imatinib treatment, suggesting that LCP1^{Ser5} phosphorylation is dependent on F/P tyrosine kinase activity (Figure 1B). To analyze whether LCP1 is critical for the survival of F/P-positive cells, three specific LCP1 shRNA constructs (shLCP1 #1, #2, and #3) and a scrambled short hairpin RNA (shRNA) control (scr) were transduced into both 32D-EV and 32D-F/P cells. In IL-3-starved 32D-EV cells, phosphorylation of target proteins was absent, while in 32D-F/P scr cells, STAT5, AKT^{Ser473}, and STAT1^{Y701} phosphorylation, as well as LCP1 protein expression, were increased (Figure 1C). As a result of LCP1 knockdown (shLCP1 clones #1, #2, and #3), phosphorylation levels of AKT^{Ser473} and STAT1^{Tyr701} were decreased, while phosphorylation of AKT^{Thr308} was increased and STAT5 remained unaltered (Figure 1C), suggesting that the activation of STAT5 by F/P is LCP1-independent. Furthermore, the proliferation of the shLCP1 knockdown cell lines was moderately but significantly reduced in comparison to 32D-F/P scr cells (Figure 1D). Reduction of STAT1^{Y701} and AKT^{Ser473} phosphorylation was confirmed in the human eosinophilia-derived F/P-positive cell line Eo1-1³⁵ when LCP1 messenger RNA (mRNA) expression was targeted by shRNA (Figure 1E, shLCP1 #2). Although reduction of LCP1 protein was

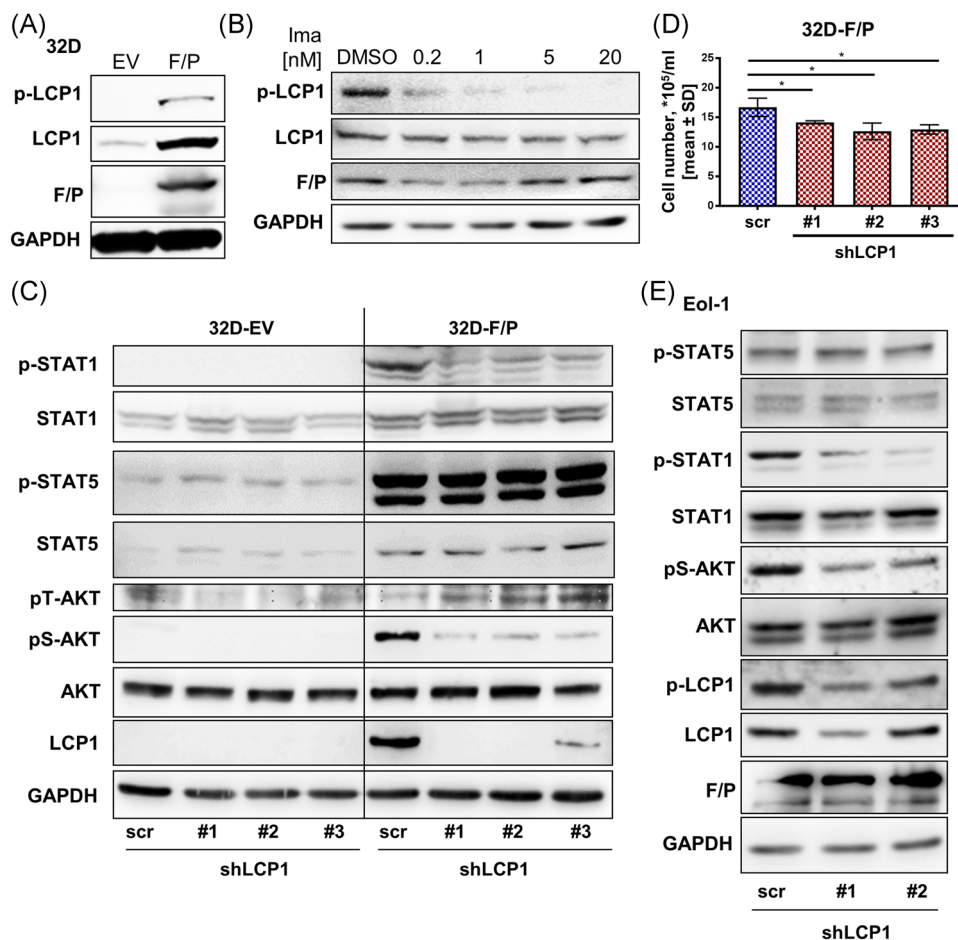


FIGURE 1 AKT and STAT1 phosphorylation downstream of Fip1L1-PDGFRa (F/P) is mediated by LCP1. A, LCP1 protein expression and Ser5 phosphorylation were analyzed in empty vector (EV) or F/P transduced 32D cells by immunoblotting. B, 32D-F/P cells were treated with imatinib (0.2, 1, 5, and 20 nM) for 16 hours. LCP1^{Ser5} phosphorylation and total LCP1 protein levels were determined by immunoblotting. C, Three different LCP1 knockdown vectors (shLCP1#1, #2, #3) as well as one scrambled control (scr) were transduced into either 32D-EV or F/P cells. LCP1 protein expression was detected to evaluate knockdown efficacy. Phosphorylation of STAT1 (Tyr701), STAT5 (Tyr694), and AKT (Thr308, Ser473) were analyzed by immunoblotting. GAPDH served as a loading control. D, 32D-F/P scr, shLCP1#1, #2, and #3 cells (2×10^5 /mL) were seeded in WEHI-3B-free medium. Cell numbers were assessed after 48 hours of cultivation and mean values \pm SD are given. * $P < .05$. E, Eol-1 cells were lentivirally transduced with two different LCP1 knockdown vectors (shLCP1#1, shLCP1#2) as well as one scrambled control (scr). Transduced cells were selected by puromycin (500 ng/mL) and cultivated with 200 ng/mL doxycycline for 72 hours. Phosphorylation and total protein levels of STAT5, AKT (Ser473), and LCP1 were analyzed by immunoblotting. GAPDH served as a loading control. GAPDH, glyceraldehyde 3-phosphate dehydrogenase; LCP1, lymphocyte cytosolic protein 1; Ser5, serine5; STAT, signal transducer and activator of transcription [Color figure can be viewed at wileyonlinelibrary.com]

not effective in shLCP1 #2 cells, phosphorylation of LCP1^{Ser5} was reduced, probably explaining the reduction of p-STAT1 and pS-AKT (Figure 1E). Again, STAT5 was not influenced by LCP1 knockdown. These data collectively link active LCP1 protein to the phosphorylation of AKT and STAT1 in F/P-positive cells. Of note, LCP1 knockdown in Eol-1 cells was not stable, suggesting that LCP1 protein is critical for malignant eosinophil cell survival.

3.2 | Enza reduces cell growth, clonogenic potential, and migration of Eol-1 cells

To confirm that LCP1 is activated by PKC β ,⁹ Eol-1 cells were exposed to increasing concentrations of the PKC β -specific

inhibitor Enza. LCP1 phosphorylation was gradually inhibited by Enza, and this inhibition was enhanced by combination with imatinib (Figure 2A). The proliferation and metabolic activity of Eol-1 cells were reduced by Enza and sotrastaurin treatment in a dose-dependent manner (Figures 2B,C and S1A). Meanwhile, no significant cell growth reduction of 32D-F/P cells was observed (Figure S1B), suggesting an eosinophil-specific effect of Enza independent from direct F/P inhibition. 32D-EV cells did not survive IL-3 deprivation. We further confirmed a significant reduction of the clonogenic growth of Enza treated Eol-1 cells (Figure 2D), which may be due to the induction of apoptosis in long time treatment. LCP1 inhibition by Enza reduced mRNA expression of the major basic protein, eosinophil-derived neurotoxin, and

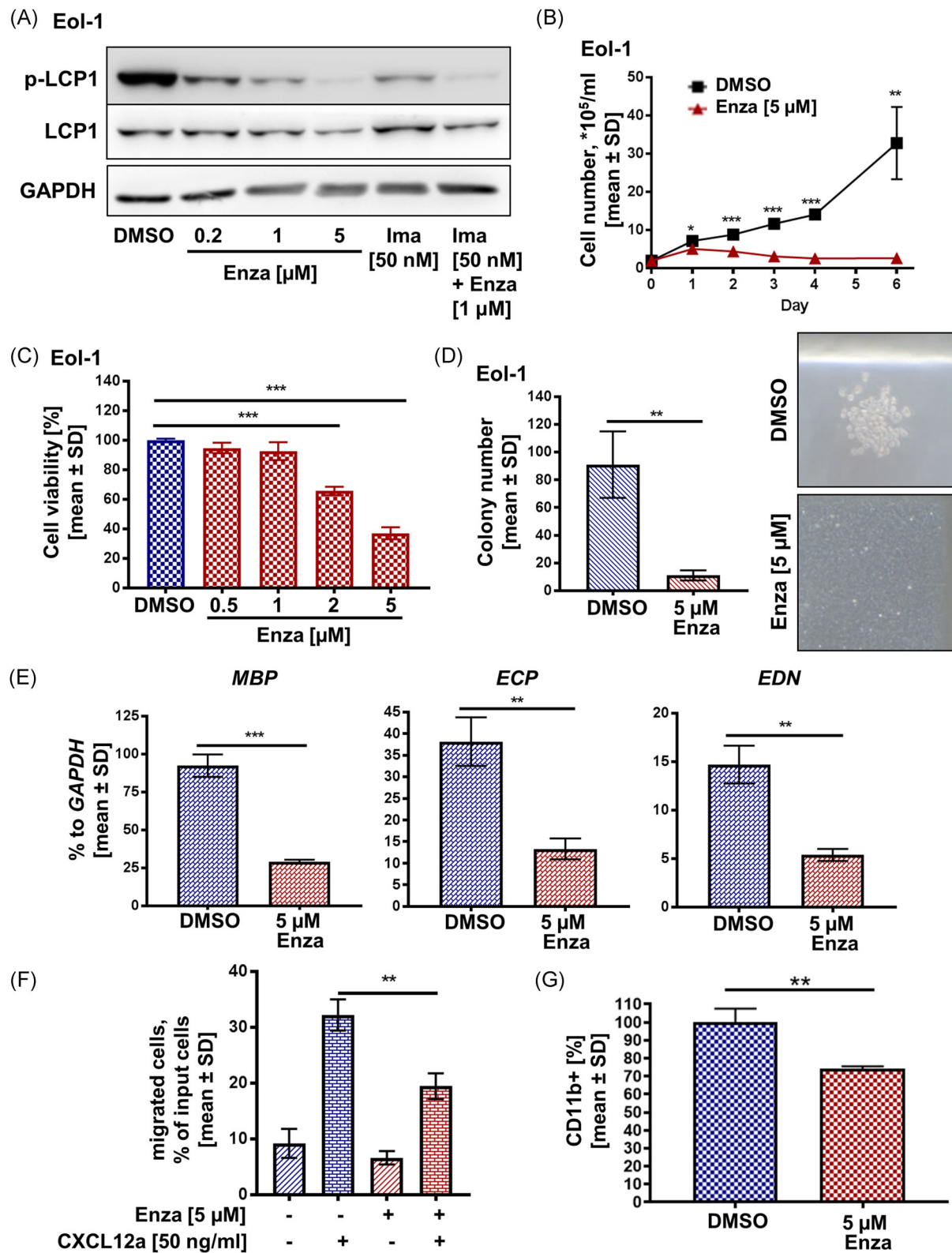


FIGURE 2 Continued.

eosinophil cationic protein and cell migration triggered by CXCL12a³⁶ (Figure 2E,F). Since CD11b is a critical mediator of eosinophil functions including migration,³⁷ we analyzed CD11b cell surface expression of Eol-1 cells. Indeed, Enza treatment significantly reduced CD11b cell surface expression (Figure 2G).

3.3 | Enza induces cell death and reduces STAT1^{Tyr701} and AKT^{Ser473} phosphorylation

Given the inhibitory effect of Enza on Eol-1 cell growth and eosinophil functions upon a short-time treatment, the induction of apoptosis was analyzed.

Enza treatment of Eol-1 cells significantly increased the percentage of nonvital cells in comparison with DMSO control (Figure 3A). In addition, PARP-1 cleavage, a hallmark of apoptosis, was detected in lysates of Enza (5 μ M) treated Eol-1 cells (Figure 3B). Enza was previously reported to induce β -catenin protein stabilization in multiple myeloma cells, with accumulated β -catenin being associated with a c-Jun-mediated increase of *TP73* expression, leading to induction of apoptosis.³⁷ We confirmed the accumulation of β -catenin and c-Jun and upregulation of *TP73* mRNA expression in Enza treated Eol-1 cells (Figure 3C,D). Thus, these data suggest a similar mechanism of Enza-induced apoptosis in multiple myeloma and HE cells.

To analyze altered signaling in Eol-1 cells due to Enza treatment, we applied increasing amounts of Enza (0.2, 1, 5 μ M) into the cell culture medium for 16 hours and generated cell lysates. Enza did not decrease the phosphorylation of STAT5, STAT3, and ERK1/2 (Figure 3E), suggesting that Enza did not inhibit F/P kinase activity directly. Importantly, phosphorylation of AKT^{Ser473} and STAT1^{Tyr701} was decreased in a dose-dependent manner upon Enza treatment, while hyperphosphorylation of AKT^{Thr308} was detected (Figure 3E), comparable with LCP1 knockdown experiments (Figures 1C and 1E). A dose-dependent loss of AKT substrate phosphorylation was observed upon Enza treatment (Figure 3F,G), demonstrating the importance of AKT^{Ser473} phosphorylation for AKT kinase activity. In addition, more direct inhibition of AKT activity by wortmannin (phosphatidylinositol 3-kinase [PI3K] inhibitor), MK2206 (AKT inhibitor) and BEZ235 (dual PI3K and mTOR inhibitor) efficiently reduced AKT^{Ser473} phosphorylation and proliferation of Eol-1 cells (Figure S2A,B,C), confirming an important role of AKT in eosinophil survival.³⁸

3.4 | LCP1 regulates AKT^{Ser473} phosphorylation via mTORC2

AKT activity is mainly regulated by Pyruvate dehydrogenase lipamide kinase isozyme 1 (PDK1), phosphorylating AKT^{Thr308}, and the mTORC2 complex, regulating phosphorylation of the residue Ser473.³⁹ Therefore, we hypothesized that LCP1, which is inactivated by Enza treatment, regulates mTORC2 activity. We demonstrate that in Eol-1 cells PDK1^{Ser241} phosphorylation, essential for PDK1 activity, was not altered by Enza treatment (Figure 4A). However, the mRNA expression levels of the mTORC2 components *Rictor* and *Deptor* were reduced (Figure 4B). It was reported that p-AKT^{Thr308} regulates the phosphorylation of AKT^{Ser473} via mTORC2 component Sin1.³⁹ Since we observed that Enza treatment and LCP1 knockdown led to dephosphorylation of AKT^{Ser473} but hyperphosphorylation of AKT^{Thr308} (Figures 3E and 4C), the activity of Sin1 was analyzed. As hypothesized, Sin1^{Thr86} was dephosphorylated in Eol-1 cells after Enza treatment (Figure 4C). Moreover, Sin1 protein expression and its phosphorylation at Thr86 were reduced by LCP1 knockdown in 32D-F/P cells (Figure 4D). Finally, we confirmed the interaction of endogenous LCP1 with mTOR and G β L, two subunits of the mTORC2 complex (Figure 4E). This interaction, although weak, decreased, if Eol-1 cells were treated with Enza. Collectively, our data indicate a critical role of LCP1 in mTORC2 complex activity, which is accordingly responsible for the phosphorylation of AKT^{Ser473}.

3.5 | LCP1 knockdown inhibits eosinophil differentiation and reduces AKT/STAT1 expression in SCF-ER-HoxB8 cells

To investigate the role of LCP1 in eosinophil differentiation in a primary cell system, immortalized murine BM progenitor cells were generated by stable expression of the *Hoxb8* gene.²⁴ In the presence of β -estradiol, these progenitor cells (SCF-ER-HoxB8 cells) remain undifferentiated, and upon removal of β -estradiol and addition of IL-5, SCF-ER-HoxB8 cells differentiate into mature eosinophils.²⁴ While DMSO-treated SCF-ER-HoxB8 cells gave rise to 11.34% (\pm 2.73%) eosinophils (Siglec-F⁺/CD11b⁺), Enza treatment significantly decreased eosinophil differentiation to 1.12% (\pm 0.42%) without

FIGURE 2 Enzastaurin inhibits cell growth, colony-forming ability and migration of Eol-1 cells. A, Eol-1 cells were treated with increasing concentrations of enzastaurin (Enza) or 50 nM imatinib (Ima) \pm 1 μ M enzastaurin for 4 hours and analyzed by immunoblotting with the indicated antibodies. B, Eol-1 cells (2×10^5 /mL) were cultured in the presence of 5 μ M enzastaurin or DMSO as control. The cell number was analyzed daily for 6 days. SD is indicated, * $P < .05$, ** $P < .01$, *** $P < .001$. C, Metabolic activity of Eol-1 cells (3×10^4 per well) was analyzed after 72 hours of enzastaurin treatment (0.5, 1, 2, and 5 μ M). MTT absorbance was measured at 550 nm. D, After DMSO (control) or 5 μ M enzastaurin pretreatment (24 hours), Eol-1 cells (500 per well) were added into cytokine free methylcellulose with 5 μ M enzastaurin or equal amount of DMSO. Colony number was counted under a light microscope at day 4. (E) Eol-1 cells (1×10^6 /mL) were subjected to 5 μ M enzastaurin for 24 hours. mRNA expression of *MBP*, *ECP*, and *EDN* was analyzed by qRT-PCR and are shown as % of *GAPDH*. (F) Eol-1 cells were pretreated with DMSO or 5 μ M enzastaurin for 24 hours. Transwell assays were then performed using 1.5×10^5 cells per well. CXCL12a (50 ng/mL) was used as a chemoattractant. Migrated cells were analyzed after 4 hours of incubation. (G) Flow cytometry analysis of CD11b cell surface expression level of Eol-1 cells was assessed after 24 hours of exposure to DMSO or 5 μ M enzastaurin. DMSO, dimethyl sulfoxide; ECP, eosinophil cationic protein; EDN, eosinophil-derived neurotoxin; GAPDH, glyceraldehyde 3-phosphate dehydrogenase; MBP, major basic protein; MTT, 3-(4,5-dimethylthiazol-2-yl)-2,5-diphenyltetrazolium bromide; qRT-PCR, quantitative reverse transcriptase-polymerase chain reaction. ** $P < .01$, *** $P < .001$ [Color figure can be viewed at wileyonlinelibrary.com]

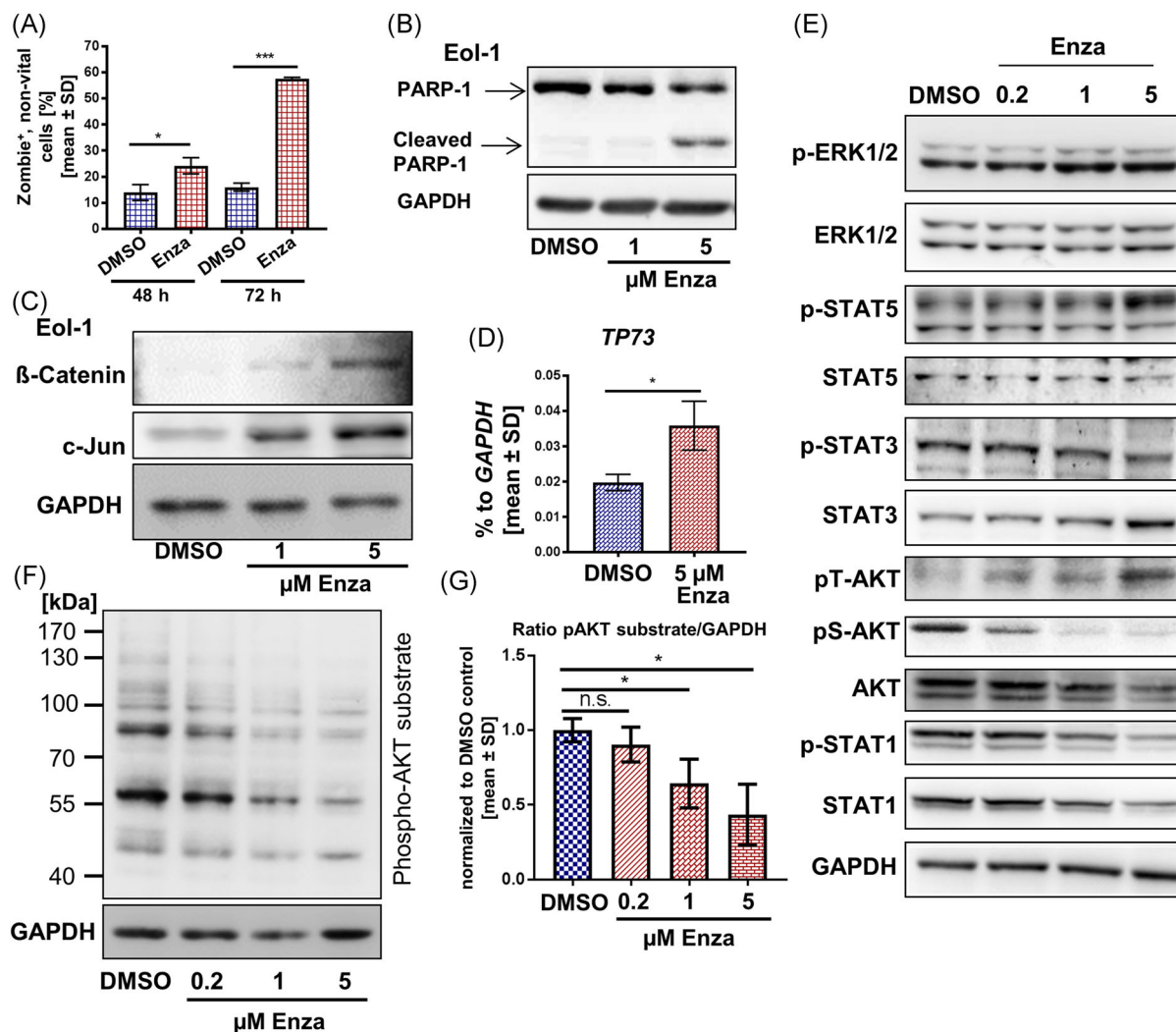


FIGURE 3 Enzastaurin induces apoptosis and reduces STAT1, AKT, and LCP1 phosphorylation in Eol-1 cells. A, Eol-1 cells (1×10^6 /mL) were subjected to 5 μ M enzastaurin (Enza). FACS analysis using Zombie Aqua staining after 48 and 72 hours incubation was used to assess nonvital cells. B, Eol-1 cells were treated with either 1 or 5 μ M enzastaurin for 16 hours and (cleaved) PARP-1 was detected by immunoblotting. GAPDH staining was used as a loading control. C, Western Blot analysis of β -Catenin, c-Jun protein expression in lysates of Eol-1 cells after 1 or 5 μ M enzastaurin treatment for 16 hours. D, Eol-1 cells were treated with enzastaurin (5 μ M) for 16 hours and RNA was isolated. *TP73* mRNA expression was analyzed by qRT-PCR. E, Eol-1 cells were treated with increasing concentrations of enzastaurin for 16 hours and analyzed by immunoblotting with the indicated antibodies. F, Lysates of DMSO or enzastaurin (0.2, 1, 5 μ M; 16 hours) treated Eol-1 cells were subjected to SDS-PAGE and immunoblotting. Phospho-AKT substrate was accessed. GAPDH served as a loading control. G, The signals from F were quantified by densitometry. The intensities of Phospho-AKT substrate versus GAPDH were calculated ($n = 3$) and normalized to DMSO control. DMSO, dimethyl sulfoxide; FACS, fluorescence activated cell sorting; GAPDH, glyceraldehyde 3-phosphate dehydrogenase; LCP1, lymphocyte cytosolic protein 1; mRNA, messenger RNA; qRT-PCR, quantitative reverse transcriptase-polymerase chain reaction; SDS-PAGE, sodium dodecyl sulfate-polyacrylamide gel electrophoresis; STAT, signal transducer and activator of transcription. SD is illustrated. * $P < .05$, ** $P < .01$ [Color figure can be viewed at wileyonlinelibrary.com]

affecting overall cell viability (Figures 5A and S3A). Furthermore, knockdown of LCP1 in SCF-ER-HoxB8-EV cells led to a significant reduction of the IL-5-driven Siglec-F⁺/CD11b⁺ double-positive eosinophil population similar to Enza treatment (Figure 5B, shLCP1#2 and shLCP1#3). In IL-5-stimulated SCF-ER-HoxB8-EV control cells, LCP1^{Ser5} phosphorylation was detectable, and knockdown was confirmed in clones #2 and #3 but not in clone #1 (Figure 5C). In keeping with this result, clones #2 and #3, but not clone #1, showed a reduction in the differentiation potential into eosinophils (Figure 5B).

We confirmed increased protein expression and phosphorylation of LCP1 in SCF-ER-HoxB8 cells stably expressing F/P (Figure 5D). In the following, LCP1 knockdown (up to 74%) was performed in SCF-ER-HoxB8-F/P cells (Figure 5E). Although the phosphorylation of STAT1^{Tyr701} and AKT^{Ser473} was not detectable in SCF-ER-HoxB8-F/P cells, the expression of both proteins was reduced, and AKT^{Thr308} phosphorylation was upregulated by LCP1 knockdown (Figure 5E). In addition, moderate but significant impairment of cell proliferation was detected in SCF-ER-HoxB8-F/P shLCP1#1, #2 and #3 cells in comparison to scr control (Figure 5F). Although SCF-ER-HoxB8-F/P

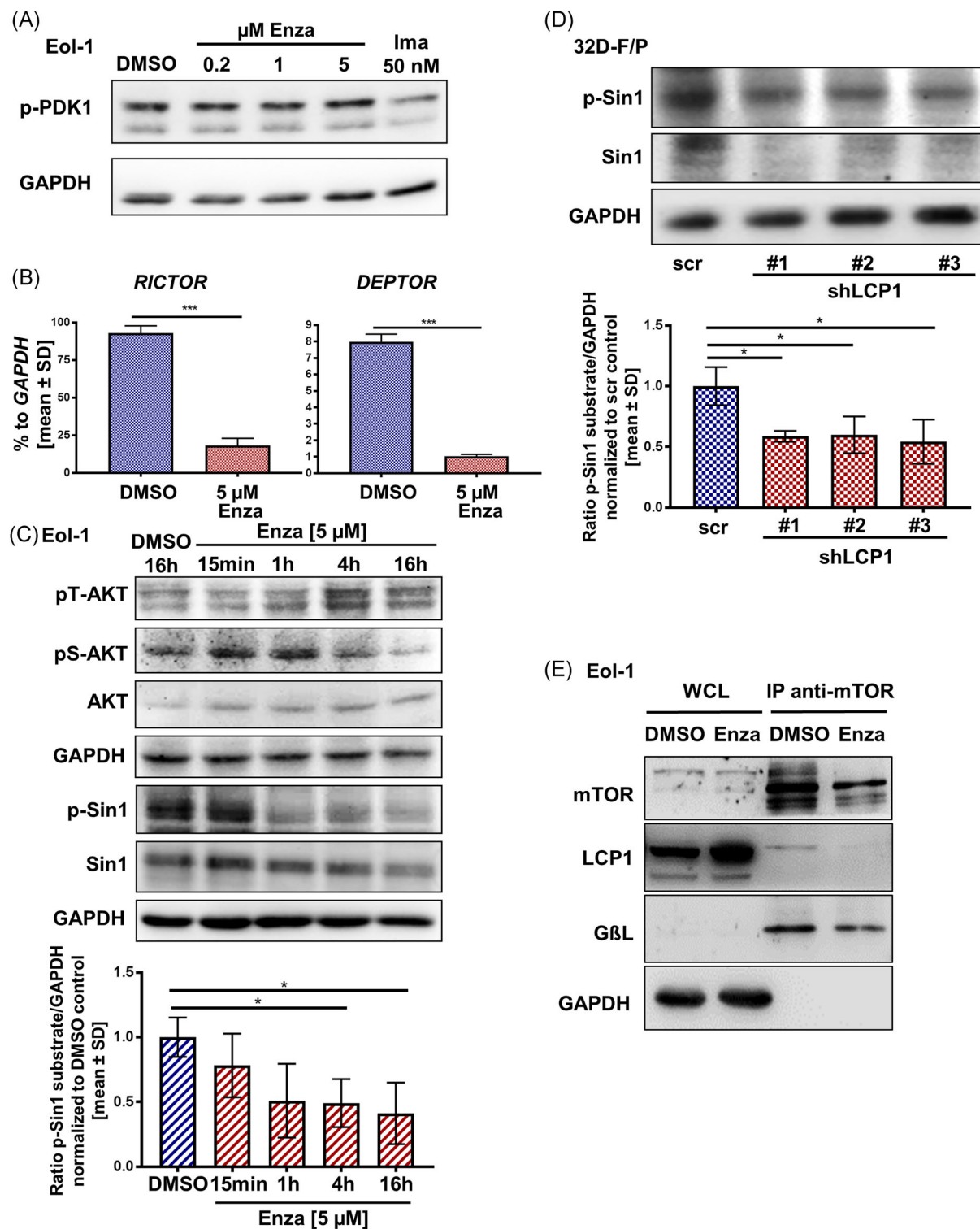


FIGURE 4 Continued.

cells were able to grow in SCF-free medium, eosinophil differentiation of SCF-ER-HoxB8-F/P cells, was not possible (Figure S3B), potentially due to the manifestation of an oncogene-dependent differentiation block.

In summary, LCP1 protein is critical for IL-5-driven eosinophil differentiation in progenitor cells of murine origin.

3.6 | Enza inhibits eosinophil differentiation of primary cells from patients with HE

In the following, peripheral blood or bone marrow samples from patients with HE were collected (Table 1), and the granulocytic population was separated over a ficoll density gradient. Cytospins and flow cytometry analysis for Siglec-8/CCR3 positivity confirmed the presence of mature eosinophils (cytospin example shown in Figure 6A,B). The percentage of mature eosinophils (Siglec-8⁺/CCR3⁺) increased during in vitro culture in the presence of IL-5 (Figure 6B). Enza treatment significantly decreased the Siglec-8⁺/CCR3⁺ cell population and overall granulocytic cell number (Figure 6B-D). MNCs of the same patients were isolated and differentiated into eosinophils in vitro for 8 to 9 days. Enza treatment significantly reduced the differentiated granulocytic cell population in comparison to the DMSO control (Figure 6E,F). In addition, a mild but significant decrease in Siglec-8 cell surface expression was observed (Figure 6G,H). Together, our data show that Enza reduces the cell number of aberrant eosinophils and partly blocks the differentiation of immature granulocytic cells into eosinophils.

4 | DISCUSSION

Most HE patients who harbor rearranged PDGFRA or PDGFRB oncogenes are sensitive to the TKI imatinib. However, only a minority of 10%-15% of HE patients carry these genetic abnormalities.¹ Currently, most of the remaining PDGFRA/PDGFRB-negative HE patients receive corticosteroids or interferon-alpha treatment with limited efficacy and significant long-term side effects, and novel treatment options are desperately needed.^{1,40}

Eosinophils have especially high amounts of actin and actin dynamic modulators important for tissue invasion and chemotaxis, priming and degranulation.^{7,8} One of these modulators, LCP1, is highly expressed in different cancer cells, implicating LCP1 as a potential biomarker,^{10,11} and we observed LCP1 to be highly expressed and phosphorylated in F/P-positive cells (Figures 1 and 2A). The knockdown of LCP1 led to a low but significant reduction of proliferation of 32D-F/P cells, while no stable LCP1 knockdown clone of Eol-1 cells could be generated, suggesting a crucial role of LCP1 in aberrant eosinophils. Interestingly, neutrophils of LCP1 knockout mice were lacking the ability to manage bacterial infections,⁴¹ while eosinophils have not been analyzed. As the establishment of stable LCP1 knockdown in Eol-1 cells was not successful and a direct link of cell loss and LCP1 protein reduction is missing, the generation of an inducible CRISPR/Cas9-driven knockout of the *Lcp1* gene is a future perspective and *lcp1* knockout mice will be a valuable tool.

PKC β II has been reported to phosphorylate LCP1 on Ser5,⁹ and we demonstrated that PKC β -specific inhibition by Enza led to LCP1 dephosphorylation. PKC proteins are activated downstream of phospholipase C γ , known to be activated by F/P and the PDGF receptors,⁴² potentially explaining the increase in LCP1^{Ser5} phosphorylation. Similar to 32D-F/P cells, BCR-ABL- as well as JAK2V617F-expressing 32D cells showed strong phosphorylation of LCP1^{Ser5}, which was inhibited by Enza treatment (Figure S4), illustrating the upregulation of LCP1^{Ser5} by different oncoproteins in myeloproliferative neoplasms (MPN) as a more general finding. Enza has been used in phase II or phase III clinical trials for the treatment of several malignant diseases, including aggressive lymphomas, glioblastoma, ovarian cancer, and lung cancer.⁴³⁻⁴⁷ Despite limited benefits shown in these tumors in a single treatment, Enza demonstrated manageable side effects and a good hematologic toxicity profile.⁴³⁻⁴⁸ Furthermore, more recent studies suggest combining Enza with ibrutinib⁴⁹ or all-trans retinoic acid⁵⁰ in diffuse large B cell lymphoma and acute promyelocytic leukemia, respectively. In the present study, Enza resulted in a significant reduction of migration, proliferation, viability, and clonogenic growth as well as induction of cell death of aberrant eosinophilic cells (Figures 2 and 3).

In eosinophils, the AKT kinase participates in eosinophil functions, such as recruitment and adhesion, and stimulates

FIGURE 4 LCP1 knockdown and enzastaurin treatment reduce p-Sin1 and mTORC2 activity. A, Eol-1 cells were incubated with different concentrations of enzastaurin (Enza) (0.2, 1, and 5 μ M) as well as 50 nM imatinib for 24 hours. PDK1 phosphorylation was analyzed by Western blot analysis. B, Eol-1 cells were subjected to either DMSO or 5 μ M enzastaurin for 24 hours and RNA was isolated. mRNA expression of *Rictor* and *Deptor* were assessed by RT-qPCR in triplicates. C, Eol-1 cells were exposed to enzastaurin (5 μ M) for the indicated time span. AKT protein expression and phosphorylation at both Ser473 and Thr308 as well as Sin1 protein expression and phosphorylation at Thr86 were accessed by Western blot analysis. The ratio of p-Sin1^{Thr86} vs GAPDH was calculated by densitometry (n = 3). D, After WEHI-3B removal overnight, Sin1 protein expression and phosphorylation at Thr86 of 32D-F/P cells transduced with either LCP1 knockdown vectors (shLCP1#1, #2, #3) or scrambled control (scr) were analyzed by Western blot analysis and quantified by densitometry. The ratio of Sin1^{Thr86} vs GAPDH was calculated (n = 3). SD is illustrated. *P < .05, **P < .01, ***P < .001. E, Eol-1 were treated with enzastaurin (5 μ M) for 16 hours and lysates were prepared. Immunoprecipitation targeting mTOR was performed and the precipitates were used for SDS-PAGE and Western blot analysis. Whole-cell lysates (WCL) were used as reference and immunostaining was performed with the indicated antibodies. DMSO, dimethyl sulfoxide; GAPDH, glyceraldehyde 3-phosphate dehydrogenase; LCP1, lymphocyte cytosolic protein 1; mRNA, messenger RNA; mTORC2, mammalian target of rapamycin complex 2; RT-qPCR, real-time quantitative reverse transcriptase-polymerase chain reaction; SDS-PAGE, sodium dodecyl sulfate-polyacrylamide gel electrophoresis [Color figure can be viewed at wileyonlinelibrary.com]

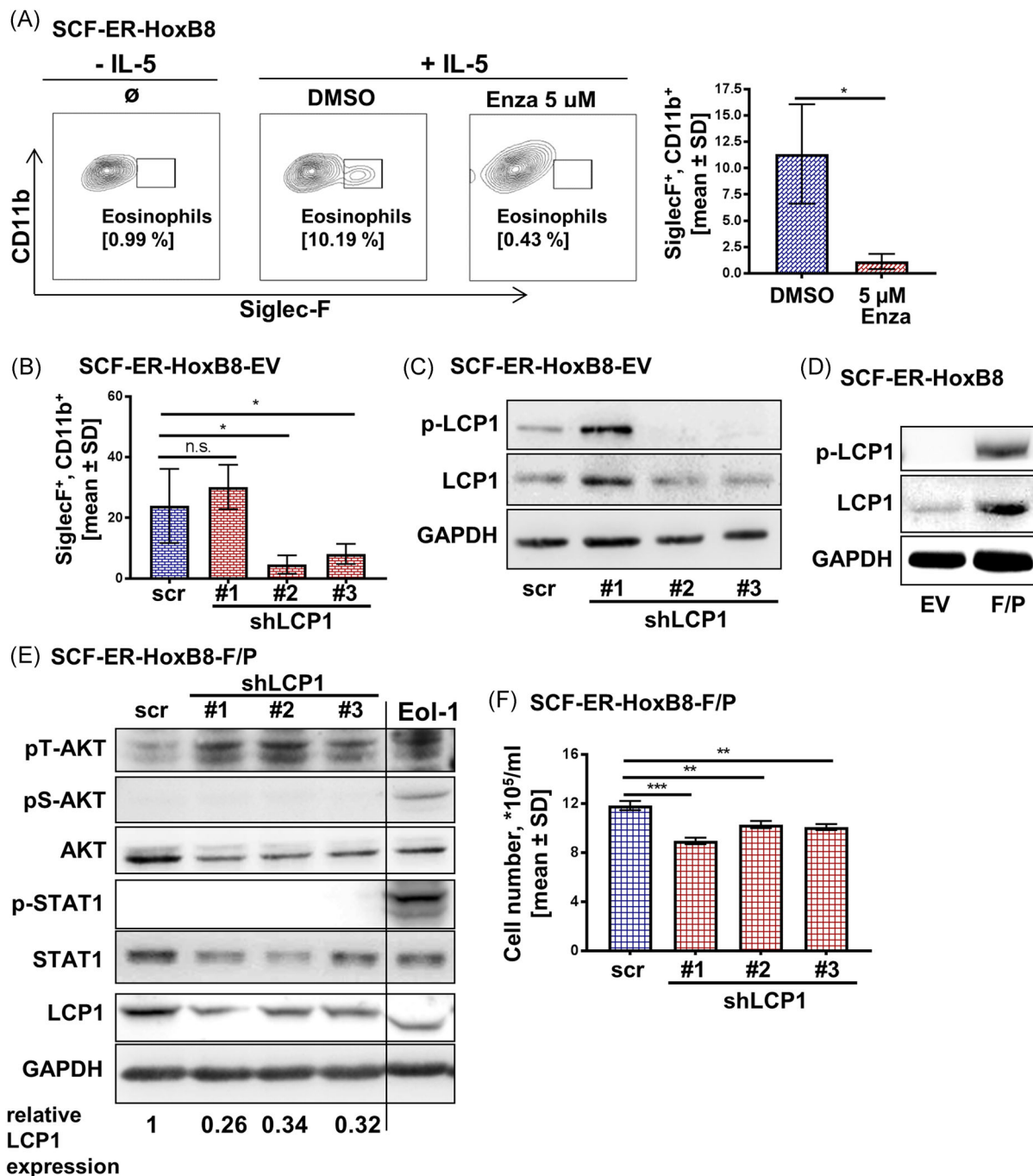


FIGURE 5 LCP1 is a critical mediator for eosinophil differentiation. A, SCF-ER-Hoxb8 immortalized BM cells were incubated with 10 ng/mL IL-5 and treated with 5 μ M enzastaurin or DMSO for 4 days upon withdrawal of β -estradiol. The parallel experiment without IL-5 stimulation was set as a negative control. Flow cytometry analysis was performed to evaluate eosinophil differentiation by Siglec-F and CD11b cell surface expression. The graph illustrates three independent experiments. SD is given. B, Immortalized SCF-ER-Hoxb8 cells were retrovirally transduced with EV or F/P. Three different shRNA constructs targeting LCP1 (shLCP1#1, #2, #3), as well as one scrambled control (scr), were retrovirally transduced into SCF-ER-Hoxb8-EV cells. EV shLCP1 cells were cultivated for 48 hours upon withdrawal of β -estradiol followed by IL-5 (10 ng/mL) stimulation for 20 minutes. The Siglec-F and CD11b double-positive population (%) of indicated SCF-ER-Hoxb8-EV cells was analyzed by flow cytometry. Means of three independent experiments and SD are given. C, SCF-ER-Hoxb8-EV cells were treated like in B. LCP1 expression and Ser5 phosphorylation were assessed by Western blot. D, p-LCP1^{Ser5} and expression levels of LCP1 were analyzed in lysates of SCF-ER-Hoxb8-EV vs SCF-ER-Hoxb8-F/P cells by Western blot analysis. E, Three different shRNA constructs targeting LCP1 (shLCP1#1, #2, #3) as well as one scrambled control (scr) were retrovirally transduced into SCF-ER-Hoxb8-F/P cells. Upon removal of β -estradiol for 2 days, LCP1 expression as well as STAT1 and AKT expression and phosphorylation levels were measured by Western blot analysis. Eo1-1 cells were used as a positive control. F, SCF-ER-Hoxb8-F/P cells (2×10^5 /mL) were subjected to IL-5 (10 ng/mL) upon removal of β -estradiol. Cell numbers were analyzed after 48 hours of cultivation by the CASY cell counter. DMSO, dimethyl sulfoxide; HoxB8, Homeobox protein Hox-B8; LCP1, lymphocyte cytosolic protein 1; SCF, stem cell factor; shRNA, short hairpin RNA; STAT signal transducer and activator of transcription. SD is illustrated. * $P < .05$, ** $P < .01$, *** $P < .001$ [Color figure can be viewed at wileyonlinelibrary.com]

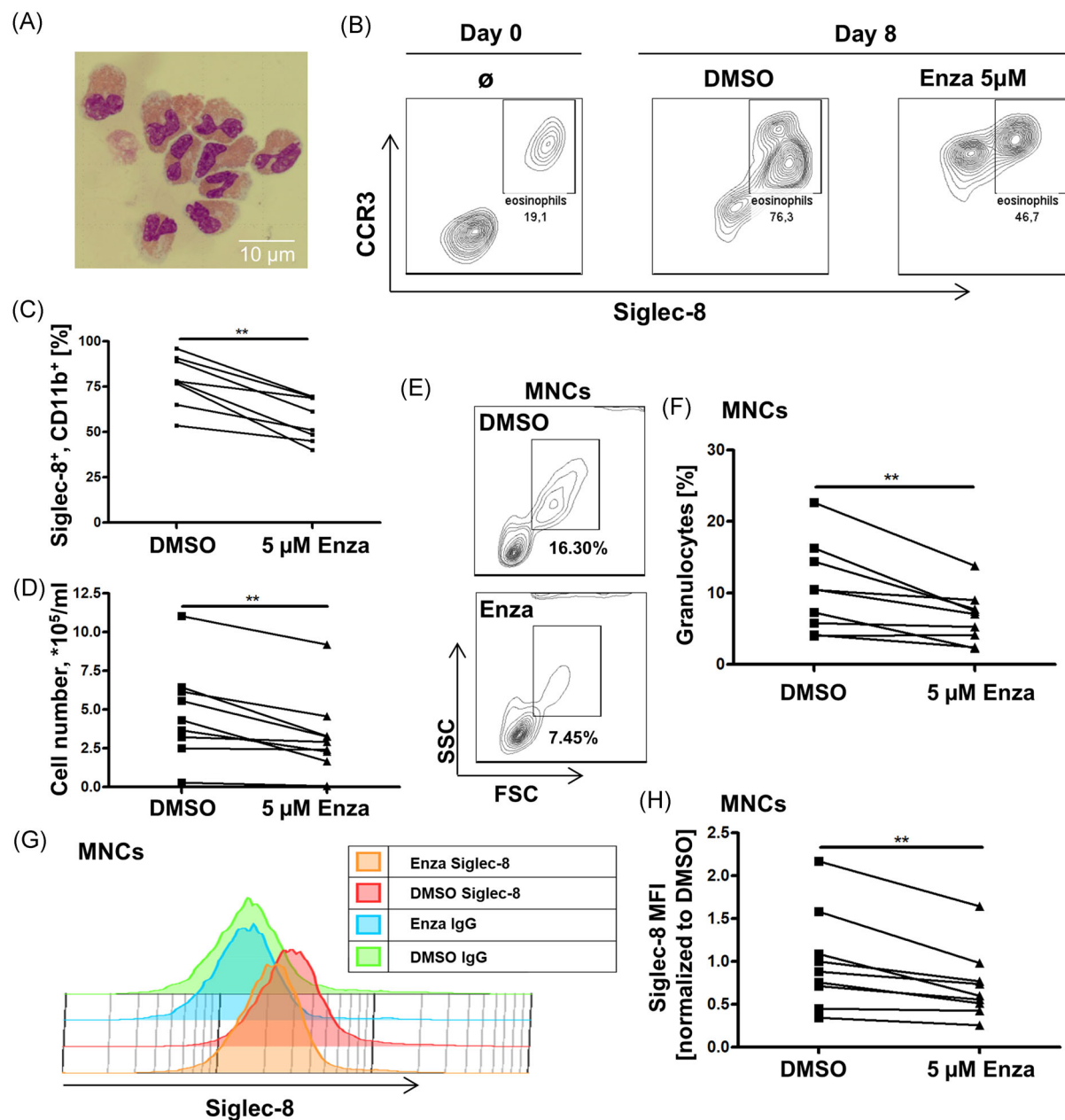


FIGURE 6 Enzastaurin treatment of HE primary samples lowers the eosinophil population and maturation. A, Peripheral blood granulocytes from HE patient were stimulated with IL-5 (10 ng/ml) for 8 days. Wright-Giemsa staining was used after cytopsin preparation. B, C, HE patient-derived peripheral blood granulocytes were stimulated with IL-5 (10 ng/mL) and subjected to 5 µM enzastaurin. Flow cytometry was performed for Siglec-8 and CCR3 double-positive cell populations between days 8 and 9. D, The granulocytic cell number of HE patients was measured by using CASY cell counter. E, F, MNCs from HE patient peripheral blood were harvested after Ficoll centrifugation. Eosinophil differentiation was initiated in media supplemented with DMSO or 5 µM enzastaurin and the granulocytic population (FSC/SSC high) was analyzed by FACS after 8 to 9 days. G, H, Siglec-8 median fluorescence intensities (MFI) of differentiated eosinophils from MNCs, cultured in DMSO or enzastaurin (5 µM) supplemented media for 8 to 9 days, were measured by FACS and normalized to DMSO control using Flowjo software. DMSO, dimethyl sulfoxide; FACS, fluorescence activated cell sorting; HE, hypereosinophilia; IL-5, interleukin-5; MNC, mononuclear cell. SD is given. ** $P < .1$ [Color figure can be viewed at wileyonlinelibrary.com]

survival.^{37,38,51} AKT is commonly regarded as a survival factor, and we demonstrate loss of viability of EoL-1 cells when AKT activity was pharmacologically targeted (Figure S2). Interestingly, only phosphorylation of AKT^{Ser473} was inhibited by Enza, in contrast to AKT^{Thr308}, which was hyperphosphorylated. In embryonic stem cells lacking PDK1, an increase of Ser473 associated with the loss of Thr308 phosphorylation was demonstrated due to higher activity of PI3K.⁵²

A similar but reciprocal mechanism in our cell system is imaginable, with increased AKT recruitment to the cell membrane in proximity to active PDK1. Accordingly, nonaltered p-PDK1 after Enza treatment was demonstrated, while phosphorylation of Sin1, part of the mTORC2 complex was reduced, which is reported to be critical for the feedback loop between the two mentioned AKT phosphorylation sites.³⁹ Furthermore, it was previously shown that the

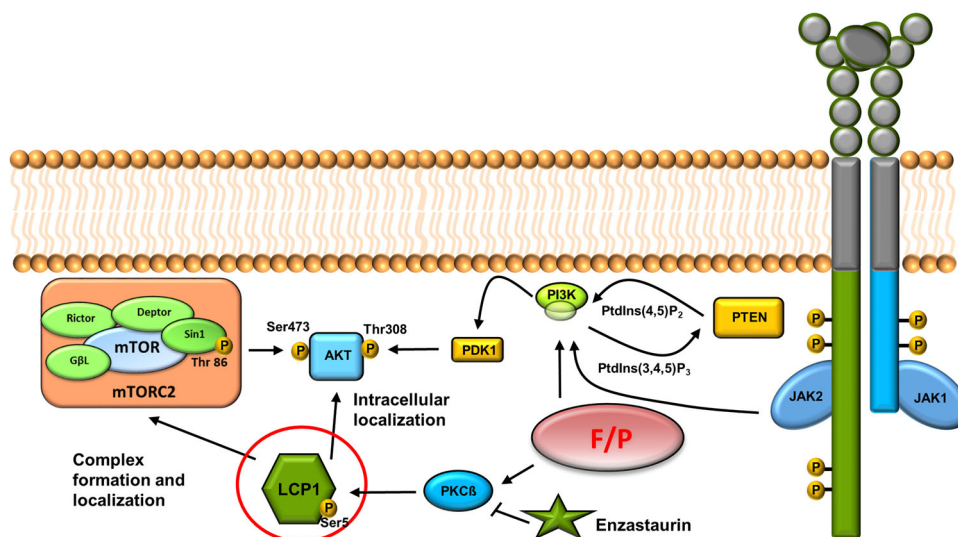


FIGURE 7 Schematic overview of the mechanism of LCP1 function in cell signaling in hypereosinophilia. LCP1, which is activated through phosphorylation at Ser5 by PKC β (downstream of the F/P oncoprotein in HES/CEL), is crucial for AKT^{Ser473} phosphorylation triggered by the mTORC2 complex. Overall AKT activity was reduced upon LCP1 knockdown or enzastaurin treatment. AKT^{Thr308} becomes hyperphosphorylated due to a potential intracellular entrapment close to active PDK1 after LCP1 protein or activity loss. Furthermore, our data suggest a role of LCP1 in complex formation and/or cellular localization of the mTORC2 complex leading to Sin1 dephosphorylation. Therefore, LCP1 may orchestrate differential signaling knots via alterations of the actin cytoskeleton in HE, blocked by enzastaurin. Cytokine receptors are depicted to illustrate a potential implication of LCP1 in e.g. IL-5 receptor complex-induced signaling. CEL, chronic eosinophilic leukemia; HE, hypereosinophilia; HES, hypereosinophilic syndrome; LCP1, lymphocyte cytosolic protein 1; mTORC2, mammalian target of rapamycin complex 2; PDK1, Pyruvate dehydrogenase lipoamide kinase isozyme 1 [Color figure can be viewed at wileyonlinelibrary.com]

ATP-competitive AKT inhibitor GDC-0068 reduced phosphorylation of Ser473 in HeLa cells, while increased phosphorylation of Thr308 was observed.⁵³ We exclude direct inhibition of AKT by Enza, as treated BCR-ABL-positive 32D cells showed no change in Ser473 phosphorylation (Figure S4B). Importantly, overall AKT activity was impaired after Enza treatment (Figure 3F,G). Although it was stated that AKT^{Ser473} is a direct target of PKC β ,⁵⁴ the cited study was performed with the multikinase inhibitor PKC412 and described downregulation of both phosphorylation sites Ser473 and Thr308,⁵⁵ clearly demonstrating a different and/or broader underlying inhibitory mechanism, probably involving LCP1.

It is currently a matter of discussion which phosphorylation sites of AKT, Thr308 or Ser473, is more crucial for AKT kinase activity,^{53,56–58} and further phosphorylation sites important for cell cycle-dependent AKT activity have come into focus.⁵⁹ A previous study demonstrated that transient phosphorylation of AKT^{Thr308} triggered by CXCL12a was impaired by siRNA targeting LCP1 in T lymphocytes.¹³ However, in F/P-positive cells we detected stronger AKT^{Thr308} but reduced AKT^{Ser473} and Sin1^{Thr86} phosphorylation by LCP1 knockdown (Figures 1C, 1E, and 4D), in line with dephosphorylation of LCP1 by Enza (Figures 3E and 4C). Likewise, in SCF-ER-HoxB8-F/P cells, AKT^{Thr308} phosphorylation was increased when LCP1 protein expression was downregulated (Figure 5E). AKT^{Ser473} phosphorylation was not detectable, probably due to specific mTORC2 activity or expression profiles in SCF-ER-HoxB8-F/P cells. Furthermore, loss of Sin1 protein in 32D LCP1 knockdown cells (Figure 4D) may be related to altered expression patterns of the six alternative Sin1 isoforms due to LCP1 protein reduction.⁶⁰ Together,

our data suggest that LCP1 is required for the activity or complex formation of mTORC2 in F/P positive cells (see Figure 7). In addition, LCP1 loss potentially influences PI3K activity or impedes dissociation of AKT from the membrane and active PDK1.

We found STAT1 to be dephosphorylated by Enza treatment and LCP1 knockdown, while STAT5 stayed unaffected. STAT5 activity is a crucial factor for survival of F/P-positive cells,⁶¹ nucleocytoplasmic shuttlings of STAT5 is described to be dependent on scaffolding proteins, such as GAB2-PI3K^{62,63} and FAK/PAK^{64,65} and serine phosphorylation of STAT5 is partly mTOR dependent.^{66,67} Although, no loss of STAT5 tyrosine phosphorylation was detected after Enza treatment, pYSTAT5 may be enriched in the cytoplasmic compartment due to LCP1 inhibition. Just recently, the STAT5 N642H was recurrently detected in myeloid neoplasms with eosinophilia.⁶⁸ The efficacy of Enza in these cases would be of future interest.

In eosinophils, STAT1 is reported to be critical for adhesion to epithelial cells by increasing intracellular adhesion molecule (ICAM) 1 expression.⁶⁹ Eosinophil migration from the blood into different tissues is a key process in HE pathogenesis.² Inhibition of PKC activity was already shown to reduce eotaxin or IL-5-triggered shape change of eosinophils.⁷⁰ We confirmed that Enza treatment reduced migration of EoL-1 cells and CD11b surface expression (Figure 2F,G). In T lymphocytes, integrin-induced cell migration towards CXCL12a is controlled by LCP1.¹³ Furthermore, B cells with LCP1 knockout demonstrate loss of CXCL12- and CXCL13-induced motility, assumably due to diminished Pyk2 signaling.⁷¹ FAK (focal adhesion kinase), like Pyk2, belongs to the FAK family of kinases which activate STAT1, and STAT1 depletion results in reduced migration.⁷² In conclusion,

loss of STAT1 phosphorylation may at least in part explain decreased eosinophil migration after either Enza treatment or LCP1 knock-down. In addition, in T cell leukemia and macrophages, STAT1 regulates inducible nitric oxide synthase expression and nitric oxide (NO) generation.⁷³ This represents a conceivable function of STAT1 in eosinophils. Further studies are needed to better define the role of LCP1 in STAT1 activation in eosinophils. Beyond migration, integrins have been shown to be essential for both eosinophil rolling and adhesion,⁷⁴ which further supports the approach of PKC and LCP1 inhibition as a potential treatment in HE.

Inhibition of differentiation is a promising clinical approach to reduce the amount of mature, hyperactive eosinophils.⁷⁵ Existing therapies targeting the key cytokine IL-5 or its receptors, such as the monoclonal antibodies mepolizumab or benralizumab, aim to achieve decreased blood eosinophilia, albeit with varying success.^{76,77} Since there is a link between LCP1 and integrin activation,^{9,71} together with our findings that shLCP1 impairs eosinophilic differentiation (Figure 5B), LCP1 presumably play a role in the IL-5 signaling pathway. This hypothesis is supported by our data demonstrating that Enza inhibits IL-5-induced eosinophil differentiation of SCF-ER-HoxB8 cells (Figure 5A), and reduces maturation and differentiation of HE patient-derived MNCs (Figure 6E,F) as well as the Ficoll-enriched granulocytic cell population (Figure 6B,C). Although most of the observed granulocytes will be eosinophils in the collected HE patient samples, it is suggestive of a general decrease of granulocytes due to Enza treatment. Meanwhile, two patient samples with MPN- or AML-associated eosinophilia carrying ABL mutations (BCR-ABL and ETV6-ABL, respectively) were treated with Enza but showed marginal loss (ETV6-ABL⁺) or even an increase in Siglec-8/CCR3 positivity (BCR-ABL⁺) (Figure S5A). The interaction between PKC β and CML is not fully understood, but PKC inhibitor treatment was described to prevent apoptosis in CML CD34⁺ cells.⁷⁸ This observation is in line with our finding, that Enza did not harm the BCR-ABL-positive cell line K562 (Figure S5B). Therefore, Enza is not expected to show clinical benefit in HE patients with ABL translocations. Just recently, high expression of LCP1 was demonstrated in multiple myeloma and its inhibition overcame proteasome inhibitor resistance,⁷⁹ again highlighting LCP1 as a worthwhile target in leukemia.

In conclusion, this study illustrates a novel application of the PKC β -specific inhibitor Enza in HE. Combinatory treatment of myeloid neoplasm with eosinophilia with Enza and JAK, PDGFR or Aurora kinase inhibitors could be an interesting topic for future analysis. Furthermore, we highlight LCP1 as a potential biomarker and a critical mediator in eosinophil differentiation as well as of mTORC2 and STAT1 activity.

ACKNOWLEDGMENTS

This study was in part supported by BILD hilft e.V. "Ein Herz für Kinder" (Research project PÄ-13311), and by the Core Facility Flow

Cytometry, a Core Facility of the Interdisciplinary Center for Clinical Research (IZKF) Aachen within the Faculty of Medicine at RWTH Aachen University. We thank Jörg Vervoorts, Institute of Biochemistry and Molecular Biology, RWTH Aachen University, for providing assistance with the coimmunoprecipitation. The pMSCV-F/P-IRES-GFP vector was a kind gift from Prof. Jan Cools, University of Leuven, Belgium. The p-LCP1^{Ser5} antibody was kindly provided by Dr. Elizabeth Schaffner-Reckinger, Université de Luxembourg, Luxembourg. pMD2.G, pRSV-Rev, and pMDLg/pRRE vectors were generated and provided by Didier Trono. Tet-pLKO-puro was obtained from Dmitri Wiederschain. Tet-pLKO-puro-scrambled was a gift from Charles Rudin. We thank Hans Haecker (St. Jude Children's Research Hospital, Memphis, TN,) for providing the MSCV-ERHBD-Hoxb8 plasmid. We thank the group of Prof. Jürgen Bernhagen, RWTH Aachen University, for providing the β -catenin antibody. Furthermore, we would like to thank the China Scholarship Council for its support. Parts of this study were generated within the medical thesis work of GM. Open access funding enabled and organized by Projekt DEAL.

CONFLICT OF INTERESTS

SK received research funding from Novartis, BMS, and Janssen (none related to this study), gave presentations and participated in advisory boards for Novartis, Pfizer, BMS, Incyte/Ariad, and Janssen. The remaining authors declare no conflict of interest. Thank you very much for your consideration.

AUTHOR CONTRIBUTIONS

GM designed the research, performed the experiments, analyzed the data, and wrote the original draft. OH and KF performed experiments and OH edited the manuscript. DG, AR, MJ, and THB contributed to the research material and edited the manuscript. MS analyzed the data and edited the manuscript. SK and NC designed the research, analyzed the data, reviewed and edited the manuscript. All authors approved the final version of the manuscript.

ORCID

Nicolas Chatain  <http://orcid.org/0000-0003-4485-3120>

REFERENCES

1. Reiter A, Gotlib J. Myeloid neoplasms with eosinophilia. *Blood*. 2017;129:704-714.
2. Rothenberg ME. Eosinophilia. *N Engl J Med*. 1998;338:1592-1600.
3. Arber DA, Orazi A, Hasserjian R, et al. The 2016 revision to the World Health Organization classification of myeloid neoplasms and acute leukemia. *Blood*. 2016;127:2391-2405.
4. Cools J, DeAngelo DJ, Gotlib J, et al. A tyrosine kinase created by fusion of the PDGFRA and FIP1L1 genes as a therapeutic target of imatinib in idiopathic hypereosinophilic syndrome. *N Engl J Med*. 2003;348:1201-1214.

5. Boehme SA, Sullivan SK, Crowe PD, et al. Activation of mitogen-activated protein kinase regulates eotaxin-induced eosinophil migration. *J Immunol*. 163:1611-1618.
6. Suzuki M, Kato M, Hanaka H, Izumi T, Morikawa A. Actin assembly is a crucial factor for superoxide anion generation from adherent human eosinophils. *J Allergy Clin Immunol*. 2003;112:126-133.
7. Starosta V, Pazdrak K, Boldogh I, Svider T, Kurosky A. Lipoxin A4 counterregulates GM-CSF signaling in eosinophilic granulocytes. *J Immunol*. 2008;181:8688-8699.
8. Straub C, Pazdrak K, Young TW, et al. Toward the proteome of the human peripheral blood eosinophil. *Proteomics Clin Appl*. 2009;3:1151-1173.
9. Pazdrak K, Young TW, Straub C, Stafford S, Kurosky A. Priming of eosinophils by GM-CSF is mediated by protein kinase C β II-phosphorylated L-plastin. *J Immunol*. 2011;186:6485-6496.
10. Shinomiya H. Plastin family of actin-bundling proteins: its functions in leukocytes, neurons, intestines, and cancer. *Int J Cell Biol*. 2012;2012:213492.
11. Foran E, McWilliam P, Kelleher D, Croke DT, Long A. The leukocyte protein L-plastin induces proliferation, invasion and loss of E-cadherin expression in colon cancer cells. *Int J Cancer*. 2006;118:2098-2104.
12. Stevenson RP, Veltman D, Machesky LM. Actin-bundling proteins in cancer progression at a glance. *J Cell Sci*. 2012;125:1073-1079.
13. Freeley M, O'Dowd F, Paul T, et al. L-plastin regulates polarization and migration in chemokine-stimulated human T lymphocytes. *J Immunol*. 2012;188:6357-6370.
14. Paclet M-H, Davis C, Kotsonis P, Godovac-Zimmermann J, Segal AW, Dekker LV. N-Formyl peptide receptor subtypes in human neutrophils activate L-plastin phosphorylation through different signal transduction intermediates. *Biochem J*. 2004;377:469-477.
15. Janji B, Giganti A, De Corte V, et al. Phosphorylation on Ser5 increases the F-actin-binding activity of L-plastin and promotes its targeting to sites of actin assembly in cells. *J Cell Sci*. 2006;119:1947-1960.
16. Ono Y, Kikkawa U, Ogita K, et al. Expression and properties of two types of protein kinase C: alternative splicing from a single gene. *Science*. 1987;236:1116-1120.
17. Kim J, Choi Y, Vallentin A, et al. Centrosomal PKC β and pericentrin are critical for human prostate cancer growth and angiogenesis. *Cancer Res*. 2008;68:6831-6839.
18. Li H, Weinstein IB. Protein kinase C β enhances growth and expression of cyclin D1 in human breast cancer cells. *Cancer Res*. 2006;66:11399-11408.
19. Murray NR, Davidson LA, Chapkin RS, Clay Gustafson W, Schattenberg DG, Fields AP. Overexpression of protein kinase C β induces colonic hyperproliferation and increased sensitivity to colon carcinogenesis. *J Cell Biol*. 1999;145:699-711.
20. Nakagawa R, Vukovic M, Tarafdar A, et al. Generation of a poor prognostic chronic lymphocytic leukemia-like disease model: PKC α subversion induces upregulation of PKC β expression in B lymphocytes. *Haematologica*. 2015;100:499-510.
21. Carnevale KA, Cathcart MK. Protein kinase C β is required for human monocyte chemotaxis to MCP-1. *J Biol Chem*. 2003;278:25317-25322.
22. Yamaguchi T, Suzuki M, Kimura H, Kato M. Role of protein kinase C in eosinophil function. *Allergol Int*. 2006;55:245-252.
23. Dickens RA, Hemann MT, Zilfou JT, et al. Probing tumor phenotypes using stable and regulated synthetic microRNA precursors. *Nat Genet*. 2005;37:1289-1295.
24. Wang GG, Calvo KR, Pasillas MP, Sykes DB, Häcker H, Kamps MP. Quantitative production of macrophages or neutrophils ex vivo using conditional Hoxb8. *Nat Methods*. 2006;3:287-293.
25. Elling C, Erben P, Walz C, et al. Novel imatinib-sensitive PDGFRA-activating point mutations in hypereosinophilic syndrome induce growth factor independence and leukemia-like disease. *Blood*. 2011;117:2935-2943.
26. Wiederschain D, Wee S, Chen L, et al. Single-vector inducible lentiviral RNAi system for oncology target validation. *Cell Cycle*. 2009;8:498-504.
27. Rudin CM, Durinck S, Stawiski EW, et al. Comprehensive genomic analysis identifies SOX2 as a frequently amplified gene in small-cell lung cancer. *Nat Genet*. 2012;44:1111-1116.
28. Dull T, Zufferey R, Kelly M, et al. A third-generation lentivirus vector with a conditional packaging system. *J Virol*. 1998;72:8463-8471.
29. Wee S, Wiederschain D, Maira S-M, et al. PTEN-deficient cancers depend on PIK3CB. *Proc Natl Acad Sci U S A*. 2008;105:13057-13062.
30. Schubert C, Allhoff M, Tillmann S, et al. Differential roles of STAT1 and STAT2 in the sensitivity of JAK2V617F- vs. BCR-ABL-positive cells to interferon alpha. *J Hematol Oncol*. 2019;12:36.
31. Wong TW, Jelinek DF. Purification of functional eosinophils from human bone marrow. *J Immunol Methods*. 2013;387:130-139.
32. Buitenhuis M, Baltus B, Lammers JJ, Coffey PJ, Koenderman L. Signal transducer and activator of transcription 5a (STAT5a) is required for eosinophil differentiation of human cord blood-derived CD34+ cells. *Blood*. 2003;101:134-142.
33. Cools J, Stover EH, Boulton CL, et al. PKC412 overcomes resistance to imatinib in a murine model of FIP1L1-PDGFR α -induced myeloproliferative disease. *Cancer Cell*. 2003;3:459-469.
34. Yamada Y, Rothenberg ME, Lee AW, et al. The FIP1L1-PDGFR α fusion gene cooperates with IL-5 to induce murine hypereosinophilic syndrome (HES)/chronic eosinophilic leukemia (CEL)-like disease. *Blood*. 2006;107:4071-4079.
35. Cools J, Quentmeier H, Huntly BJP, et al. The EOL-1 cell line as an in vitro model for the study of FIP1L1-PDGFR α -positive chronic eosinophilic leukemia. *Blood*. 2004;103:2802-2805.
36. Nagase H, Miyamasu M, Yamaguchi M, et al. Expression of CXCR4 in eosinophils: functional analyses and cytokine-mediated regulation. *J Immunol*. 2000;164:5935-5943.
37. Raab MS, Breitkreutz I, Tonon G, et al. Targeting PKC: a novel role for beta-catenin in ER stress and apoptotic signaling. *Blood*. 2009;113:1513-1521.
38. Pinho V, Souza DG, Barsante MM, et al. Phosphoinositide-3 kinases critically regulate the recruitment and survival of eosinophils in vivo: importance for the resolution of allergic inflammation. *J Leukoc Biol*. 2005;77:800-810.
39. Yang G, Murashige DS, Humphrey SJ, James DE. A positive feedback loop between Akt and mTORC2 via SIN1 phosphorylation. *Cell Rep*. 2015;12:937-943.
40. Gotlib J. World Health Organization-defined eosinophilic disorders: 2015 update on diagnosis, risk stratification, and management. *Am J Hematol*. 2015;90:1077-1089.
41. Chen H, Mocsai A, Zhang H, et al. Role for plastin in host defense distinguishes integrin signaling from cell adhesion and spreading. *Immunity*. 2003;19:95-104.
42. Demoulin J, Montano-Almendras CP. Platelet-derived growth factors and their receptors in normal and malignant hematopoiesis. *Am J Blood Res*. 2012;2:44-56.
43. Crump M, Leppä S, Fayad L, et al. Randomized, double-blind, phase III trial of enzastaurin versus placebo in patients achieving remission after first-line therapy for high-risk diffuse large B-cell lymphoma. *J Clin Oncol*. 2016;34:2484-2492.
44. Butowski N, Chang SM, Lamborn KR, et al. Phase II and pharmacogenomics study of enzastaurin plus temozolomide during and gliosarcoma. *Neuro Oncol*. 2011;13:1331-1338.
45. Wick W, Puduvalli VK, Chamberlain MC, et al. Phase III study of enzastaurin compared with lomustine in the treatment of recurrent intracranial glioblastoma. *J Clin Oncol*. 2010;28:1168-1174.
46. Chiappori A, Bepler G, Barlesi F, et al. Phase II, double-blinded, randomized study of enzastaurin plus pemetrexed as second-line

- therapy in patients with advanced non-small cell lung cancer. *J Thorac Oncol.* 2010;5:369-375.
47. Usha L, Sill MW, Darcy KM, et al. A Gynecologic Oncology Group phase II trial of the protein kinase C-beta inhibitor, enzastaurin and evaluation of markers with potential predictive and prognostic value in persistent or recurrent epithelial ovarian and primary peritoneal malignancies. *Gynecol Oncol.* 2011;121:455-461.
 48. Bourhill T, Narendran A, Johnston RN. Enzastaurin: a lesson in drug development. *Crit Rev Oncol Hematol.* 2017;112:72-79.
 49. He Y, Li J, Ding N, et al. Combination of Enzastaurin and Ibrutinib synergistically induces antitumor effects in diffuse large B cell lymphoma. *J Exp Clin Cancer Res.* 2019;38:86.
 50. Liang C, Ding M, Weng X, et al. Combination of enzastaurin and ATRA exerts dose-dependent dual effects on ATRA-resistant acute promyelocytic leukemia cells. *Am J Cancer Res.* 2019;9:906-926.
 51. Sano M, Leff AR, Myou S, et al. Regulation of interleukin-5-induced beta2-integrin adhesion of human eosinophils by phosphoinositide 3-kinase. *Am J Respir Cell Mol Biol.* 2005;33:65-70.
 52. Williams MR, Arthur JS, Balendran A, et al. The role of 3-phosphoinositide-dependent protein kinase 1 in activating AGC kinases defined in embryonic stem cells. *Curr Biol.* 2000;10:439-448.
 53. Yang J, Cron P, Thompson V, et al. Molecular mechanism for the regulation of protein kinase B/Akt by hydrophobic motif phosphorylation. *Mol Cell.* 2002;9:1227-1240.
 54. Rizvi Ma, Ghias K, Davies KM, et al. Enzastaurin (LY317615), a protein kinase Cbeta inhibitor, inhibits the AKT pathway and induces apoptosis in multiple myeloma cell lines. *Mol Cancer Ther.* 2006;5:1783-1789.
 55. Tenzer A, Zingg D, Rocha S, et al. The phosphatidylinositol 3'-kinase/Akt survival pathway is a target for the anticancer and radiosensitizing agent PKC412, an inhibitor of protein kinase C. *Cancer Res.* 2001;61:8203-8210.
 56. Vincent EE, Elder DJE, Thomas EC, et al. Akt phosphorylation on Thr308 but not on Ser473 correlates with Akt protein kinase activity in human non-small cell lung cancer. *Br J Cancer.* 2011;104:1755-1761.
 57. Gallay N, Dos Santos C, Cuzin L, et al. The level of AKT phosphorylation on threonine 308 but not on serine 473 is associated with high-risk cytogenetics and predicts poor overall survival in acute myeloid leukaemia. *Leukemia.* 2009;23:1029-1038.
 58. Sarbassov DD, Guertin DA, Ali SM, Sabatini DM. Phosphorylation and regulation of Akt/PKB by the rictor-mTOR complex. *Science.* 2005;307:1098-1101.
 59. Liu P, Begley M, Michowski W, et al. Cell-cycle-regulated activation of Akt kinase by phosphorylation at its carboxyl terminus. *Nature.* 2014;508:541-545.
 60. Ebner M, Sinkovics B, Szczygieł M, Ribeiro DW, Yudushkin I. Localization of mTORC2 activity inside cells. *J Cell Biol.* 2017;216:343-353.
 61. Buitenhuis M, Verhagen LP, Cools J, Coffey PJ. Molecular mechanisms underlying FIP1L1-PDGFRα-mediated myeloproliferation. *Cancer Res.* 2007;67:3759-3766.
 62. Harir N, Pecquet C, Kerényi M, et al. Constitutive activation of Stat5 promotes its cytoplasmic localization and association with PI3-kinase in myeloid leukemias. *Blood.* 2007;109:1678-1686.
 63. Chatain N, Ziegler P, Fahrenkamp D, et al. Src family kinases mediate cytoplasmic retention of activated STAT5 in BCR-ABL-positive cells. *Oncogene.* 2013;32:3587-3597.
 64. Chatterjee A, Ghosh J, Ramdas B, et al. Regulation of Stat5 by FAK and PAK1 in oncogenic FLT3- and KIT-driven leukemogenesis. *Cell Rep.* 2014;9:1333-1348.
 65. Berger A, Hoelbl-Kovacic A, Bourgeois J, et al. PAK-dependent STAT5 serine phosphorylation is required for BCR-ABL-induced leukemogenesis. *Leukemia.* 2014;28:629-641.
 66. Bartalucci N, Calabresi L, Balliu M, et al. Inhibitors of the PI3K/mTOR pathway prevent STAT5 phosphorylation in JAK2V617F mutated cells through PP2A/CIP2A axis. *Oncotarget.* 2017;8:96710-96724.
 67. Mitra A, Ross JA, Rodriguez G, Nagy ZS, Wilson HL, Kirken RA. Signal transducer and activator of transcription 5b (Stat5b) serine 193 is a novel cytokine-induced phospho-regulatory site that is constitutively activated in primary hematopoietic malignancies. *J Biol Chem.* 2012;287:16596-16608.
 68. Cross NCP, Hoade Y, Tapper WJ, et al. Recurrent activating STAT5B N642H mutation in myeloid neoplasms with eosinophilia. *Leukemia.* 2019;33:415-425.
 69. Profita M, Sala A, Bonanno A, et al. Cysteinyl leukotriene-1 receptor activation in a human bronchial epithelial cell line leads to signal transducer and activator of transcription 1-mediated eosinophil adhesion. *J Pharmacol Exp Ther.* 2008;325:1024-1030.
 70. Choi EN, Choi MK, Park C-S, Chung IY. A parallel signal-transduction pathway for eotaxin- and interleukin-5-induced eosinophil shape change. *Immunology.* 2003;108:245-256.
 71. Todd EM, Deady LE, Morley SC. The actin-bundling protein I-plastin is essential for marginal zone B cell development. *J Immunol.* 2011;187:3015-3025.
 72. Xie B, Zhao J, Kitagawa M, et al. Focal adhesion kinase activates Stat1 in integrin-mediated cell migration and adhesion. *J Biol Chem.* 2001;276:19512-19523.
 73. Uddin S, Sassano A, Deb DK, et al. Protein kinase C-delta (PKC-delta) is activated by type I interferons and mediates phosphorylation of Stat1 on serine 727. *J Biol Chem.* 2002;277:14408-14416.
 74. Barthel SR, Johansson MW, McNamee DM, Mosher DF. Roles of integrin activation in eosinophil function and the eosinophilic inflammation of asthma. *J Leukoc Biol.* 2008;83:1-12.
 75. Menzies-Gow A, Flood-Page P, Sehmi R, et al. Anti-IL-5 (mepolizumab) therapy induces bone marrow eosinophil maturational arrest and decreases eosinophil progenitors in the bronchial mucosa of atopic asthmatics. *J Allergy Clin Immunol.* 2003;111:714-719.
 76. Flood-Page P, Swenson C, Faierman I, et al. A study to evaluate safety and efficacy of mepolizumab in patients with moderate persistent asthma. *Am J Respir Crit Care Med.* 2007;176:1062-1071.
 77. Gotlib J. World Health Organization-defined eosinophilic disorders: 2017 update on diagnosis, risk stratification, and management. *Am J Hematol.* 2017;92:1243-1259.
 78. Pellicano F, Copland M, Jorgensen HG, Mountford J, Leber B, Holyoake TL. BMS-214662 induces mitochondrial apoptosis in chronic myeloid leukemia (CML) stem/progenitor cells, including CD34+38- cells, through activation of protein kinase Cbeta. *Blood.* 2009;114:4186-4196.
 79. Bosseler M, Marani V, Broukou A, et al. Inhibition of HIF1α-dependent upregulation of phospho-I-plastin resensitizes multiple myeloma cells to frontline therapy. *Int J Mol Sci.* 2018;19:1-18.

SUPPORTING INFORMATION

Additional supporting information may be found online in the Supporting Information section.

How to cite this article: Ma G, Gezer D, Herrmann O, et al. LCP1 triggers mTORC2/AKT activity and is pharmacologically targeted by enzastaurin in hypereosinophilia. *Molecular Carcinogenesis.* 2020;59:87-103. <https://doi.org/10.1002/mc.23131>